EPJ Web of Conferences will be set by the publisher
DOI: will be set by the publisher

Correlations and ridge in pPb collisions in the LHCb Experiment

Mariusz Witek[1,a] on behalf of the LHCb Collaboration

[1] *Institute of Nuclear Physics PAS, Cracow, Poland*

Abstract. The LHCb experiment, besides its main programme concerning flavour physics performs also very well as a general purpose forward detector, covering the pseudo-rapidity range from 2.0 to 5.0. Exploiting the experiment's unique geometry, the LHCb collaboration is pursuing a rich programme of forward QCD measurements. In particular two-particle angular correlations are studied in proton-lead collisions at a nucleon-nucleon centre-of-mass energy of $\sqrt{s_{NN}} = 5$ TeV, with data collected by the LHCb detector at the LHC in 2013. The analysis is based on data recorded in two opposing beam configurations, in which either the direction of the proton or that of the lead remnants is analysed. This is the first measurement of a long-range correlation on the near side in proton-lead collisions in the forward region. It extends previous observations in the central region.

1 Introduction

The two-particle angular correlations are one of the tools to study the dynamics of multi-particle production in QCD and to probe collective effects arising in the dense environment of a high-energy collision. They are usually described by two-dimensional $(\Delta\eta, \Delta\phi)$-correlation functions measured in the laboratory system. The two ranges can be distinguished, the short-range ($|\Delta\eta| \lesssim 2$) and long-range ($|\Delta\eta| \gtrsim 2$) effects. On the near-side ($|\Delta\phi| \approx 0$) a short-range "jet-peak" at $\Delta\eta \approx 0$ is the dominant structure. It is caused by the fact that in the fragmentation process, the final-state particles are collimated around the initial parton. To balance the momentum, the peak is accompanied by a long-range structure on the away side ($|\Delta\phi| \approx \pi$) caused by particles that fly opposite in azimuthal angle. The near side long range correlations in the form of the so called ridge effect have been seen at the Relativistic Heavy-Ion Collider (RHIC)in p+Au and Au+Au collisions [1, 2]. Surprisingly, it turned out that in the high multiplicity class of proton-proton interactions the ridge has been also found by CMS [3]. Later, the ridge effect was reported for p+Pb collisions by Alice [4], Atlas [5] and CMS [6]. The theoretical interpretation of the mechanism responsible for the ridge in small colliding system like proton-proton is still under discussion. Various models have been proposed including colour reconnection and gluon saturation in the framework of a colour-glass condensate [7–10] or the hydrodynamic evolution of a high density partonic medium [11], multiparton interactions [12–14], jet-medium interactions [15, 16], and collective effects [17–21] induced by the formation and expansion

[a] e-mail: mariusz.witek@ifj.edu.pl

of a high-density system likely produced in these collisions. The instrumentation of the LHCb single-arm spectrometer covers a unique rapidity range $2 < \eta < 5$ in the laboratory frame [22, 23]. The measurements are based on proton-lead collisions that are dominated by single interactions (98%). The two beam configurations provided by LHC, p+Pb and Pb+p which differs by the direction of proton and ion beams can be analysed in the forward region. The simple trigger was configured to accept events with at least one reconstructed track in the vertex detector for non-empty beam bunch crossing. The events were required to have exactly one reconstructed primary vertex with at least five tracks. The tracks were selected to originate directly from interaction point based on its impact parameter with respect to primary vertex. The effect of fake tracks after track quality cuts imposed and the track reconstruction efficiency is taken into account as a weight assigned to each track. The analysis is based on a subset of the total data set recorded during the 2013 pPb running period, $0.46\,\mathrm{nb}^{-1}$ in the p+Pb configuration and $0.30\,\mathrm{nb}^{-1}$ for the Pb+p configuration. The rapidity range in the nucleon-nucleon centre-of-mass frame is $1.5 < y < 4.4$ for p+Pb and $-5.4 < y < -2.5$ for Pb+p. The results of the analysis were published in Ref. [24].

2 Analysis method

The particles are divided into three subsets according to their p_{T}: $0.15 - 1.0\,\mathrm{GeV}/c$, $1.0 - 2.0\,\mathrm{GeV}/c$ and $2.0 - 3.0\,\mathrm{GeV}/c$, and analysed separately. The analysis method follows the standard approach formulated e.g. in Ref. [25]. All particles in a given subset are taken as a trigger particle one by one. All other particles are combined with the trigger particle in a pair. Two correlation functions are constructed. The signal one $S(\Delta\eta, \Delta\phi)$ for pairs from the same event and $B(\Delta\eta, \Delta\phi)$ for pairs combined from mixed events. The correlation function reads:

$$\frac{1}{N_{\mathrm{trig}}} \frac{\mathrm{d}^2 N_{\mathrm{pair}}}{\mathrm{d}\Delta\eta\,\mathrm{d}\Delta\phi} = \frac{S(\Delta\eta, \Delta\phi)}{B(\Delta\eta, \Delta\phi)} \times B(0,0), \tag{1}$$

where N_{pair} is the number of particle pairs found in a $(\Delta\eta, \Delta\phi)$ bin and N_{trig} is the number of trigger particles and $B(0,0)$ is the normalization factor. By construction, the effects due to the detector occupancy, acceptance and material are accounted for by dividing the signal by the background distribution, where the latter is normalised to unity around the origin.

Since the two-particle correlations are strongly dependent on the total number of particles produced in collision, the analysis is performed for various classes of event activity. The p+Pb and Pb+p minimum bias samples each consist of about 1.1×10^8 events which are randomly selected from about 10 times larger full sample. The high-multiplicity samples contain all available events with at least 2200 hits in the vertex detector and amount to about 1.1×10^8 events in p+Pb and 1.3×10^8 events in Pb+p collisions. Five event-activity classes are defined as fractions of the hit-multiplicity distributions of the minimum-bias samples, as indicated in Fig. 1. Since collisions recorded in the Pb+p configuration reach larger hit-multiplicities compared to those in the p+Pb configuration, the relative classes are defined separately for each configuration. The 50 – 100% class contains 50% of events with the lowest event activities, followed by the 30 – 50% and 10 – 30% classes representing medium-activity events, and the 0 – 10% and 0 – 3% classes of high-activity events. The event multiplicities seen in the detector for two beam configurations are different. In order to compare the results, five common absolute activity classes (five bins labeled I – V) were defined. They are listed in Table 1. A scaling factor was introduced to achieve the same total event multiplicity in the same bin for p+Pb and Pb+p configurations.

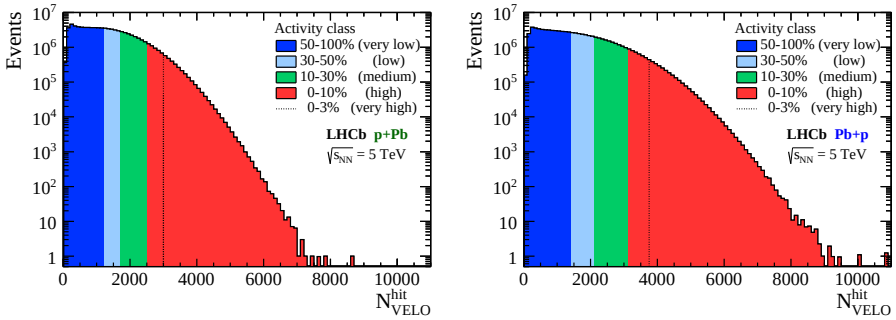

Figure 1. Hit-multiplicity distribution in the vertex detector for selected events of the minimum-bias samples in the (left) p+Pb and (right) Pb+p configurations. The activity classes are defined as fractions of the full distribution, as indicated by colours (shades). The 0 – 3% class is a sub-sample of the 0 – 10% class. The figures were taken from Ref. [24].

Table 1. Common absolute activity bins for the p+Pb and Pb+p samples. The activity of p+Pb events is scaled to match the same activity ranges of Pb+p events, as explained in the text. For illustration purposes the average number, $\langle N_{ch}\rangle_{\rm MC}$, of prompt charged particles with $p > 2\,{\rm GeV}/c$, $p_{\rm T} > 0.15\,{\rm GeV}/c$ and $2.0 < \eta < 4.9$ is listed for events simulated with the HIJING event generator.

Common absolute activity bin	$N^{\rm hit}_{\rm VELO}$-range in Pb+p scale	p+Pb $\langle N_{ch}\rangle_{\rm MC}$	Pb+p $\langle N_{ch}\rangle_{\rm MC}$
Bin I	2200 – 2400	62.8 ± 6.6	64.4
Bin II	2400 – 2600	68.4 ± 7.1	67.0
Bin III	2600 – 2800	73.7 ± 7.6	76.4
Bin IV	2800 – 3000	79.2 ± 7.9	82.4
Bin V	3000 – 3500	86.7 ± 8.2	92.9

3 Results

The correlation for particles with $1 < p_{\rm T} < 2\,{\rm GeV}/c$ is illustrated in Fig. 2 for p+Pb configuration and in Fig. 3 for Pb+p configuration. The near-side peak around $\Delta\eta = \Delta\phi = 0$ is truncated in the histograms. For low activity events only the jet-peak is observed while for highest activity class a clear ridge effect emerges. It is more pronounced in the case of Pb+p sample.

The detailed study of the evolution of the long-range correlations on the near and away sides is usually performed in one dimensional projections integrated over $\Delta\eta$:

$$Y(\Delta\phi) \equiv \frac{1}{N_{\rm trig}}\frac{{\rm d}N_{\rm pair}}{{\rm d}\Delta\phi} = \frac{1}{\Delta\eta_b - \Delta\eta_a}\int_{\Delta\eta_a}^{\Delta\eta_b}\frac{1}{N_{\rm trig}}\frac{{\rm d}^2N_{\rm pair}}{{\rm d}\Delta\eta{\rm d}\Delta\phi}{\rm d}\Delta\eta. \quad (2)$$

The jet-peak area is excluded by averaging the two-dimensional yield over the interval from $\Delta\eta_a = 2.0$ to $\Delta\eta_b = 2.9$. The non interesting correlations in the form of flat pedestals in the yield are subtracted using the zero-yield-at-minimum (ZYAM) method [26]. The subtracted one-dimensional yields for the p+Pb (full circles) and Pb+p (open circles) data samples are shown in Fig. 4 for all activity classes and $p_{\rm T}$ intervals. It can be seen that the correlation strength increases with event activity on the near side, but decreases towards higher $p_{\rm T}$ where fewer particles are found. Since more particles are emitted into the acceptance of the detector in the Pb+p compared to the p+Pb configuration, a

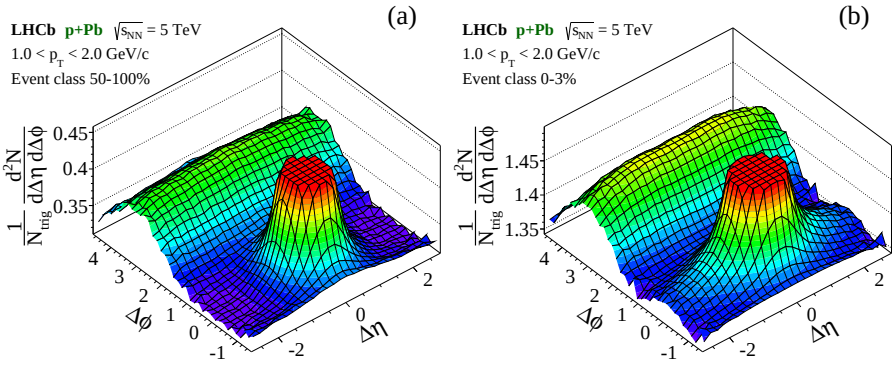

Figure 2. Two-particle correlation functions for events recorded in the p+Pb configuration, showing the (a) low and (b) high event-activity classes. The figures were taken from Ref. [24].

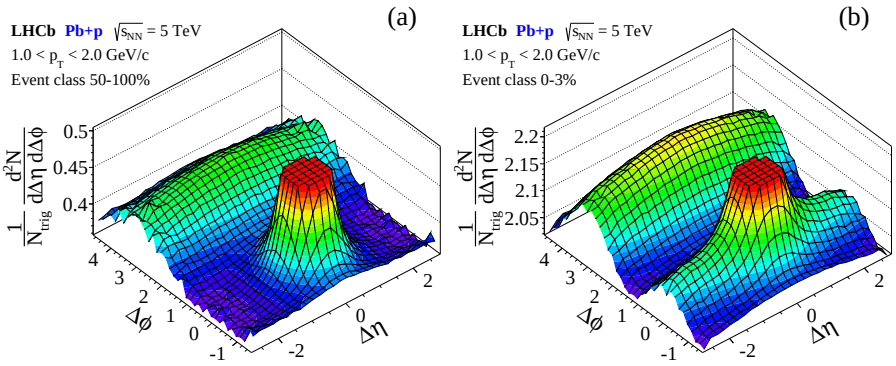

Figure 3. Two-particle correlation functions for events recorded in the Pb+p configuration, showing the (a) low and (b) high event-activity classes. The figures were taken from Ref. [24].

larger offset is observed, as indicated by the ZYAM constants. In the highest-activity class, 0 − 3%, the near-side ridge is strongly pronounced in all p_{T} intervals for both Pb+p and p+Pb samples. The ridge effect decreases with decreasing event activity and disappears for the activity class 30 − 50%. For p+Pb the near-side peak is significantly lower.

Similar ZYAM-subtracted yields for common bins of absolute activity are presented in Fig. 5 for $1 < p_{\mathrm{T}} < 2\,\mathrm{GeV}/c$. The results for the p+Pb and Pb+p samples are compared in five event classes which probe identical activities in the range of $2.0 < \eta < 4.9$. The measured hit-multiplicities of the p+Pb sample are scaled to agree with the hit-multiplicities of the Pb+p sample. It turns out that the observed long-range correlations become compatible for p+Pb and Pb+p.

4 Summary

The samples of pPb collisions at $\sqrt{s_{NN}} = 5\,\mathrm{TeV}$ collected by the LHCb experiment were used to study two-particle angular correlations for the first time in the forward region covering the pseudorapidity range $2.0 < \eta < 4.9$ in the laboratory frame. The observation of the ridge in the forward region extends

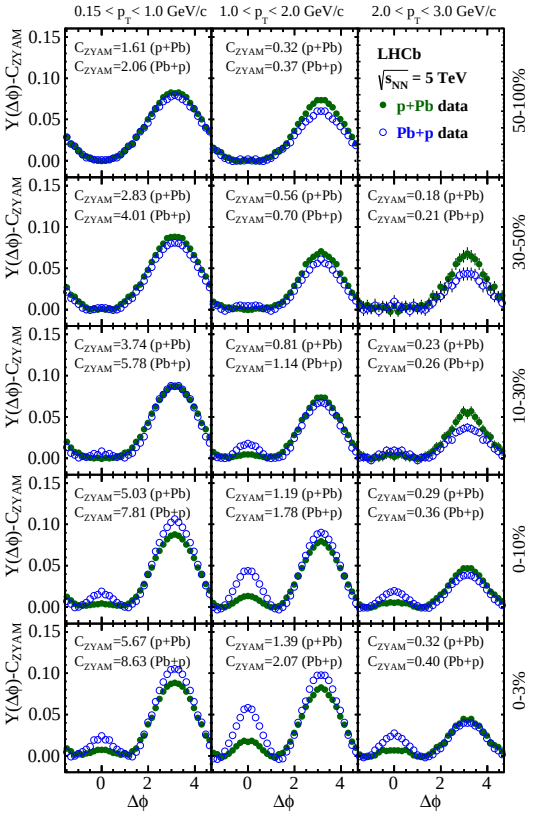

Figure 4. One-dimensional correlation yield as a function of $\Delta\phi$ obtained from the ZYAM-method by averaging over $2.0 < \Delta\eta < 2.9$. The figure was taken from Ref. [24].

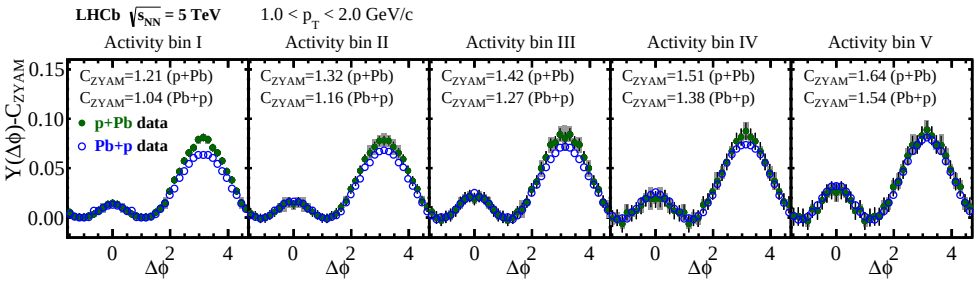

Figure 5. One-dimensional correlation yield as a function of $\Delta\phi$ obtained from the ZYAM-method by averaging the two-dimensional distribution over $2.0 < \Delta\eta < 2.9$. The figure was taken from Ref. [24].

previous LHC measurements. The analysis was performed separately for the p+Pb and Pb+p beam configurations probing the rapidities in the nucleon-nucleon centre-of-mass frame of $1.5 < y < 4.4$ and $-5.4 < y < -2.5$, respectively. The analysis was performed in various p_{T} ranges and for different event activity classes. In high event activity class, a long-range correlation on the near side (the ridge) is observed in both configurations. The near-side ridge is most pronounced in the range $1 < p_{\mathrm{T}} < 2\,\mathrm{GeV}/c$. For identical absolute activity ranges in the p+Pb and Pb+p configurations the observed long-range correlations are compatible.

Acknowledgements

I would like to express my gratitude to the National Science Centre NCN in Poland, for financial support under the contract no. 2013/11/B/ST2/03829.

References

[1] B. Abelev et al., Phys. Rev. **C80**, 064912 (2009).
[2] B. Alver et al., Phys. Rev. Lett. **104**, 062301 (2010).
[3] Khachatryan, V., Sirunyan, A.M. et al., CMS collaboration, J. High Energ. Phys. (2010) 91.
[4] B. Abelev et al., ALICE Collaboration, Phys. Lett. **B719**, 29 (2013)
[5] G. Aad et al., ATLAS Collaboration, Phys. Rev. Lett. **110**, 182302 (2013)
[6] S. Chatrchyan et al., CMS Collaboration, Phys. Lett. **B718**, 795 (2013)
[7] Dusling, Kevin and Venugopalan, Raju, Phys.Rev. **D87**, 051502 (2013)
[8] Dusling, Kevin and Venugopalan, Raju, Phys.Rev. **D87**, 054014 (2013)
[9] Dusling, Kevin and Venugopalan, Raju, Phys.Rev. **D87**, 094034 (2013)
[10] Kovchegov, Yuri V. and Wertepny, Douglas E., Nucl.Phys. **A906**, 50-83 (2013)
[11] Bzdak, Adam and Schenke, Bjoern and Tribedy, Prithwish and Venugopalan, Raju, Phys.Rev. **C87**, 064906 (2013)
[12] Alderweireldt, Sara and Van Mechelen, Pierre, Proceedings of the 3rd International Workshop on Multiple Partonic Interactions at the LHC (MPI@LHC 2011), 33-40 (2012)
[13] Strikman, Mark, Acta Phys.Polon. **B42**, 2607-2630 (2011)
[14] Ryskin, M.G. and Martin, A.D. and Khoze, V.A., J.Phys. **G38**, 085006 (2011)
[15] Hwa, Rudolph C. and Yang, C.B., Phys.Rev. **C83**, 024911 (2011)
[16] Wong, Cheuk-Yin, Phys.Rev. **C84**, 024901 (2011)
[17] Avsar, Emil and Flensburg, Christoffer and Hatta Yoshitaka and Ollitrault, Jean-Yves and Ueda, Takahiro, Phys.Lett., **B702**,394-397 (2011)
[18] Werner, K. and Karpenko, Iu. and Pierog, T., Phys.Rev.Lett. **106**, 122004 (2011)
[19] Bozek, Piotr, Phys. Rev. **C85**, 014911 (2012)
[20] Bozek, Piotr and Broniowski, Wojciech, Phys.Lett. **B718**,1557-1561 (2013)
[21] Shuryak, Edward and Zahed, Ismail, Phys.Rev. **C88**, 044915 (2013)
[22] Alves Jr., A. A. and others, LHCb collaboration, JINST**3**, S08005 (2008)
[23] Aaij, R. and others, LHCb collaboration, Int. J. Mod. Phys. **A30**, 1530022 (2015)
[24] Aaij, R. and others, LHCb collaboration, Phys. Lett. **B762** 473-483 (2016)
[25] Abelev, Betty and others, ALICE collaboration, Phys.Lett. **B719**, 29-41 (2013)
[26] Ajitanand, N. N. and Alexander, J. M. and Chung, P. and Holzmann, W. G. and Issah, M. and Lacey, Roy A. and Shevel, A. and Taranenko, A. and Danielewicz, P., Phys. Rev. C **72**, 011902 (2005)